

MULTI-FREQUENCY GROUND-PENETRATING RADAR SURVEYS OF TEPHRA AND BURIED ICE AT ASKJA VOLCANO, NORTHERN ICELAND. E. S. Shoemaker¹, D. M. H. Baker², J. A. Richardson², S. P. Scheidt^{2,3}, L. M. Carter¹, P. L. Whelley^{2,4}, and K. E. Young², ¹Lunar and Planetary Laboratory, University of Arizona, Tucson, AZ (eshoemaker@email.arizona.edu), ²NASA Goddard Space Flight Center, Greenbelt, MD, ³Howard University, Washington, DC, ⁴University of Maryland, College Park, MD

Introduction: From 2010-2016, it was estimated that ~7% of the land area of Iceland was underlain by permafrost [1]. This permafrost maintains a tenuous stability at higher altitude mountainous regions like Askja Volcano located in the Northern Icelandic highlands (Fig. 1) [2]. Eruptions in March, 1875 [3] and October-November, 1961 [4] deposited rhyolitic pumice and basaltic lapilli, respectively, onto a layer of fresh snowfall. Later, massive ice was likely formed through a combination of compaction, meltwater refreeze, and ice aggradation [5].

This ice buried beneath unvegetated, unconsolidated tephra is potentially analogous to some ice deposits within regolith and pyroclasts at the Moon and Mars [6]. Ground-penetrating radar (GPR) is a powerful tool for the near-surface exploration of Earth and planetary bodies and can be used by future robotic and human missions to detect and characterize subsurface water ice. Our GPR investigations of ice layers and their volcanoclastic overburden at Askja provide insight into the evolving permafrost conditions at high altitude volcanic sites in Iceland [1,2,5]. Our work also provides an assessment of observational, analytical, and operational methods that may be transferrable to future surface missions on Mars and the Moon where identifying shallow subsurface (0-10 m) water ice is an important human and robotic exploration objective [7,8].

Methodology: GPR surveys of buried ice deposits in the eastern portion of the Askja caldera were collected during two field campaigns in July/August 2019 and August 2021 using Geophysical Survey Systems Inc. (GSSI) shielded GPR antennas. We conducted a total of 102 surveys in the caldera at 200, 400, and 900 MHz center frequencies. These frequencies allowed us to map the ice at various penetration depths and resolutions. Radar traces were recorded at a rate of 100/m triggered by an attached wheel odometer. A mounted GPS was used for geopositioning. Buried ice was confirmed along the GPR traverses using a hammer drill and auger to bore to depths of 1-1.5 m or by digging trenches. Aerial imagery surveys were also conducted during each field campaign over each survey site using an uncrewed aerial vehicle (UAV) to document geomorphic surface expressions of buried ice coincident with GPR survey traces (Fig. 2).

Estimating Attenuation. Gains and losses to the radar signal are described by the radar equation, which includes attenuation [see 9]. We processed the radar traces by applying a horizontal background filter to remove any coherent noise that could be masking reflectors and performed a Hilbert transform to further reduce noise. We

isolated attenuation at each center frequency by averaging traces across sections of our collected radargrams where the reflectors are not varying substantially with depth. We then corrected this average trace for the backscatter cross-sections of the reflecting target along with the geometric spreading of the wave front as it propagates radially through the subsurface. We assumed our subsurface interfaces are smooth reflecting targets and so the radar equation was simplified to a model-dependent gain function of the form $1/R^2$, where R is depth in m, applied to the average trace. We then applied a linear least-squares fit to the portion of the corrected average trace exhibiting an exponential decay with depth to estimate the total two-way attenuation, or loss-rate, in dB/m [10] (Fig. 3). We used this total attenuation to test our hypothesis that regions where ice is buried beneath tephra exhibit a lower loss rate compared to ice-free regions.

Results and Interpretations: We observed laterally extensive massive ice deposits beneath both the 1875 pumice and 1961 tephra throughout the caldera (Figs. 1 & 2). Many deposits are correlated with thermokarst and permafrost landforms. Between the 2019 and 2021 campaigns, new ablation features were observed indicating the degradation of these ice deposits is increasing as the climate warms [11].

GPR Stratigraphy. At each frequency, we resolved both the top and bottom of ice layers as bright, continuous reflectors resulting from interfaces between the overlying tephra and underlying, older volcanic deposits (Fig. 2). Small amounts of perched meltwater at the top of the ice layers led to minor dielectric enhancement. Samples beneath the 1875 pumice in the southern and eastern portions of the caldera exhibited interstitial ice between tephra grains at ~15-20 cm depth and pure ice at depths of 0.6-1 m with thicknesses ranging between 0.8-2.5 m. Other ice deposits were as thin as 7 cm, but as thick as 1.9 m in some places buried beneath ~0.4-0.5 m of the 1961 tephra (Fig. 2).

GPR Attenuation. We measured low two-way loss rates for regions where ice is buried beneath 1875 pumice or 1961 tephra as well as for ice-free regions (Fig. 3). Sites with 1875 pumice had a higher loss rate compared to the 1961 tephra likely due to the larger clast sizes and scattering cross-section of the pumice compared with the basaltic lapilli. This scattering behavior was visually evident in the collected radargrams at those sites. At 200 MHz, we measured a loss rate of 0.25 dB/m for ice buried by 1875 pumice, 0.17 dB/m for ice buried by 1961 tephra, and we measure 0.34 dB/m

for an ice-free region of 1875 pumice burying the 1961 lava flow. We find similar trends at 400 MHz.

Conclusions: Our GPR surveys in 2019 and 2021 throughout the Askja caldera successfully identified shallow layers of tephra from the 1875 and 1961 eruptions and widespread massive ice deposits. Many ice deposits were associated with thermokarst and permafrost landforms and hummocky terrain. New ablation features were identified over a two-year period indicating that ice stability is tenuous.

The attenuation properties between ice-rich and ice-free regions appear to be different. At 200 and 400 MHz, we found generally low loss rates associated with ice-rich regions of the caldera. Fitting of GPR data at other sites to estimate loss rates at these frequencies and at 900 MHz are currently ongoing. Our work in Iceland suggests that multi-frequency GPR attenuation analysis may be important for identifying subsurface ice in planetary missions where complementary boreholes, trenches, or other measurements of the subsurface are not possible [12].

Acknowledgments: This work was supported by the Goddard Instrument Field Team as a part of the 2019/2021 Volcanic Deposit Evolution and Origins (VIDEO) expeditions. We thank the Vatnajökull National Park for their support and permission to carry out this work.

References: [1] Czekirka J. et al. (2019) *Frontiers in Earth Sci.*, 7, 130.[2] Etzelmüller B. et al. (2020) *Quaternary Sci. Rev.*, 233, 106236.[3] Carey R. J. et al. (2010) *Bull. Volc.*, 72(3), 259–278.[4] Thorarinsson, S. and Sigvaldason, G. E. (1962) *Am. J. Sci.*, 260, 641–651.[5] Kellerer-Pirklbauer A. (2007) *Permafrost and Periglacial Proc.*, 18(3), 269–284.[6] Campbell B. A. et al. (2021) *JGR* 126(3) e2020JE006601.[7] MEPAG ICE-SAG Final Report (2019) <http://mepag.nasa.gov/reports/cfm>. [8] LEAG (2016) The Lunar Exploration Roadmap, <https://www.lpi.usra.edu/leag/roadmap/>. [9] Annan A. P. & Davis J. L. (1977) *Geol. Soc. Can. Rep. Activ. B, Pap.*, 77-1B, 117–124. [10] Grimm R. E. et al. (2006) *JGR*, 111(E6). [11] Hart J. et al. (2021) *EGU Gen. Asm. Conf. Abstracts*. EGU21-8411. [12] Hamran S. et al. (2020) *Space Sci. Rev.* 216(8) 128.

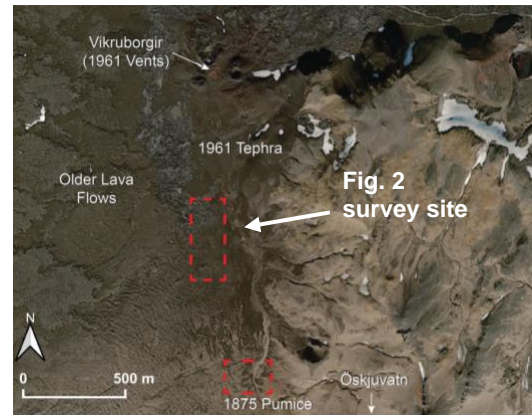


Fig. 1. Basaltic lapilli deposited in 1961 within the Askja caldera drapes over buff colored 1875 pumice to the south toward the caldera lake Öskjuvatn. Locations of GPR survey sites are shown as red boxes.

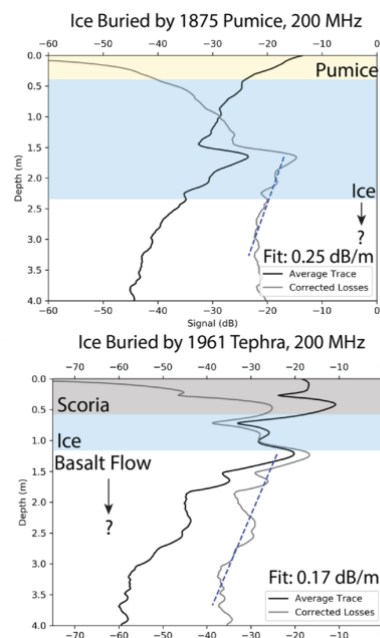


Fig. 3. Average 200 MHz traces (black line). The lower panel corresponds to the observation shown in Fig. 2. Linear fits (blue dashed line) of the corrected average trace (grey line) yields two-way loss rates in dB/m over a range of depths where the signal exhibits an exponential decay. Losses are higher in the 1875 pumice regions, likely due to scattering of the signal by the larger clasts.

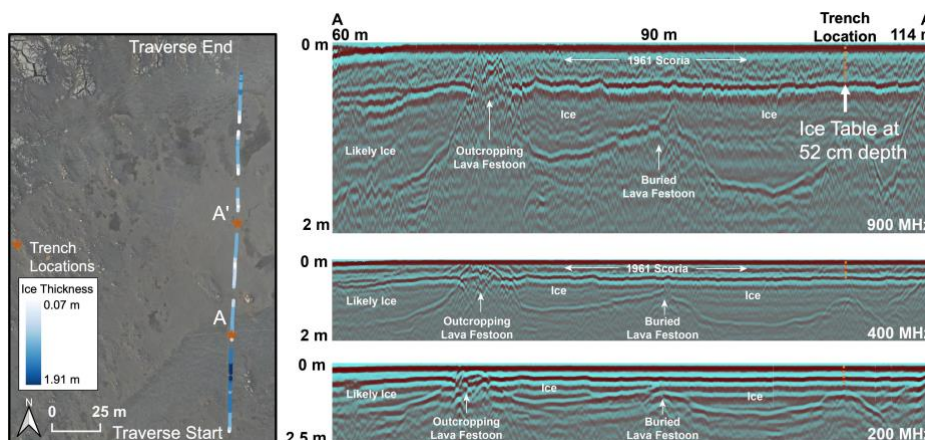


Fig. 2. A ~200 m long GPR traverse taken over 1961 tephra burying massive ice that has formed in troughs between basaltic lava festoons (left panel). The panels on the right are 900 MHz (top), 400 MHz (middle), and 200 MHz (bottom) radargrams. The overlying tephra, ice layers, and lava festoons are labeled. The top of the ice table was determined to be at 52 cm depth from a trench (orange stars, orange dashed lines). Ice thicknesses were estimated using a dielectric constant of 3.62 at 400 MHz.